

ANNALS OF GLACIOLOGY



CAMBRIDGE
UNIVERSITY PRESS

THIS MANUSCRIPT HAS BEEN SUBMITTED TO THE ANNALS OF GLACIOLOGY AND HAS NOT BEEN PEER-REVIEWED.

A Scenario-Neutral Approach to Climate Change in Glacier Mass Balance Modelling

Journal:	<i>Annals of Glaciology</i>
Manuscript ID	Draft
Manuscript Type:	Article
Date Submitted by the Author:	n/a
Complete List of Authors:	van der Laan, Larissa; Leibniz University Hannover, Cholibois, Kim; Leibniz University Hannover El Menuawy, Ayscha; Leibniz University Hannover Forster, Kristian; Leibniz University Hannover
Keywords:	Glacier mass balance, Glacier modelling, Climate change
Abstract:	In hydrology and water resources management, scenario-neutral methods are already common, mostly used to rapidly compare system responses to plausible changes in climate. As a first application in glaciology, a scenario-neutral approach, using climatic mass balance as a system response, is applied to four glaciers: Hintereisferner (AT), Peyto Glacier (CA), Austre Brøggerbreen (NO) and Abramov Glacier (KGZ). The Open Global Glacier Model (OGGM) is used to perform a scenario-neutral glacier sensitivity analysis, resulting in visual, two-dimensional response surfaces, and a glacier sensitivity index (GSI). In addition, four Coupled Model Intercomparison Project Phase 6 models (CMIP6) (FGOALS3, MPI-ESM1, EG-Earth 3, NorESM2), under four Shared Socioeconomic

	<p>Pathways (SSP) (1-2.6, 2-4.5, 3-7.0, 5-8.5) are overlaid, for comparison. Assessing results shows that overall, Hintereisferner is most sensitive to changes in climate overall, and temperature especially, with a temperature GSI of 1.12 m w.e./°C - 1.96 m w.e./°C, versus, for example, a temperature GSI of 0.56 m w.e./°C - 0.81 m w.e./°C for Peyto glacier. Seasonally, we see differences in sensitivity between climatic variables and glaciers, too. Overlaying time slices of the CMIP6 models emphasizes how scenario-neutral approaches are suitable for use in glacier modelling, especially as a framework for sensitivity studies.</p>

SCHOLARONE™
Manuscripts

A Scenario-Neutral Approach to Climate Change in Glacier Mass Balance Modelling

Larissa VAN DER LAAN,¹ Kim CHOLIBOIS,¹ Ayscha EL MENUAWY,¹ Kristian FÖRSTER,¹

¹ *Institute for Hydrology and Water Resources Management, Leibniz Universität Hannover, Hannover, Germany*

Correspondence: Larissa van der Laan <vdlaan@iww.uni-hannover.de>

ABSTRACT. In hydrology and water resources management, scenario-neutral methods are already common, mostly used to rapidly compare system responses to plausible changes in climate. As a first application in glaciology, a scenario-neutral approach, using climatic mass balance as a system response, is applied to four glaciers: Hintereisferner (AT), Peyto Glacier (CA), Austre Brøggerbreen (NO) and Abramov Glacier (KGZ). The Open Global Glacier Model (OGGM) is used to perform a scenario-neutral glacier sensitivity analysis, resulting in visual, two-dimensional response surfaces, and a glacier sensitivity index (GSI). In addition, four Coupled Model Intercomparison Project Phase 6 models (CMIP6) (FGOALS3, MPI-ESM1, EG-Earth 3, NorESM2), under four Shared Socioeconomic Pathways (SSP) (1-2.6, 2-4.5, 3-7.0, 5-8.5) are overlaid, for comparison. Assessing results shows that overall, Hintereisferner is most sensitive to changes in climate overall, and temperature especially, with a temperature GSI of 1.12 m w.e./°C - 1.96 m w.e./°C, versus, for example, a temperature GSI of 0.56 m w.e./°C - 0.81 m w.e./°C for Peyto glacier. Seasonally, we see differences in sensitivity between climatic variables and glaciers, too. Overlaying time slices of the CMIP6 models emphasizes how scenario-neutral approaches are suitable for use in glacier modelling, especially as a framework for sensitivity studies.

26 INTRODUCTION

27 Glacier mass change is of global interest, as it influences sea level, ecosystem hydrology, and is of significant
28 importance for the water needs of communities downstream (Brighenti and others, 2019; Milner and others,
29 2017; Zemp and others, 2019). Glacier melt was the largest contributor to sea level rise over the 20th
30 Century, and is projected to remain a significant contributor throughout the 21st Century (Farinotti and
31 others, 2019; Frederikse and others, 2020; Marzeion and others, 2017; Slangen and others, 2017). In
32 addition, glaciers' water storage capacity make their monitoring and prediction crucial to water resources
33 management (Förster and van der Laan, 2022; Ultee and others, 2022; Jansson and others, 2003). With
34 their surface mass balance predominantly governed by changes in precipitation and temperature, a robust
35 understanding of glacier sensitivity to climate change is essential in making predictions for the future
36 (Singh and others, 2018). Traditionally, predicting 21st Century glacier mass loss is done using a 'top-
37 down' approach, forcing glacier models with regional climates, directly or indirectly derived from General
38 Circulation Models (GCM), yielding glacier mass evolution under imposed scenarios, see e.g. Hock and
39 others (2019) for a comprehensive overview.

40 However, with much of the manifestation of specific climate change scenarios being shaped by socio-
41 economic and political development, there are significant uncertainties in the estimates of scenario like-
42 lihoods (Kemp and others, 2022; Reilly and others, 2001). This scenario uncertainty dominates sources
43 of uncertainty in glacier model projections over decision-relevant timescales (Hinkel and others, 2019;
44 Marzeion and others, 2020). In order to gain an understanding of system responses to a plausible range
45 of potential changes in climate, regardless of exact scenario and its inherent uncertainty, the development
46 of scenario-neutral approaches has been increasingly active over the past decade (Culley and others, 2021;
47 Guo and others, 2017). Especially in hydrology and water resources management, with an emphasis on
48 extreme events such as floods and droughts, 'bottom-up' approaches, using a number of scenario-neutral
49 methods, are being utilized (e.g. Beylich and others, 2021; Guo and others, 2018; Keller and others, 2019;
50 Prudhomme and others, 2010). Essential in these studies is the identification of and focus on the climate
51 variables to which the system is most sensitive (Guo and others, 2017). In the case of climatic glacier mass
52 balance, these variables are clearly identifiable as precipitation and temperature (Oerlemans and Reichert,
53 2000). These variables form the base for the widely used mass balance model type 'temperature index
54 model', which assumes an empirical relationship - with a physical basis (Ohmura, 2001) - between melt

55 and temperature. Adding an approximation of the ratio of precipitation that falls in solid form, approxi-
56 mating accumulation, yields a model estimate of glacier mass balance. The term mass balance, as used in
57 this study, refers to the climatic or 'reference surface' mass balance Elsberg and others (2001), calculated
58 over a fixed geometry, focusing solely on the influence of changes in climate.

59 The aim of the current study is to use a scenario-neutral approach on four case-study glaciers, located
60 in different climatic zones. We estimate overall and seasonal glacier sensitivity to plausible changes in
61 climate, expressed through glacier mass balance. The resulting response surfaces offer a framework in which
62 to analyze and compare critical system thresholds and explore the timing of pre-defined climate change
63 scenarios. We showcase the latter by superimposing the results from a traditional top-down approach,
64 using four Coupled Model Intercomparison Project Phase 6 (CMIP6) models, driven with four Shared
65 Socioeconomic Pathways (SSP), on the response surfaces.

66 **STUDY AREA**

67 For the purpose of highlighting the differences in climate sensitivity between glaciers, we look at four
68 glaciers in different climatic zones: Hintereisferner (AT), Peyto Glacier (CA), Austre Brøggerbreen (NO)
69 and Abramov Glacier (KGZ), see figure 1. All four glaciers are World Glacier Monitoring Service (WGMS)
70 reference glaciers, meaning they have an observational record of more than 30 years, and are largely
71 governed by climatic factors, rather than debris cover, calving or surging (WGMS, 2022b; Wijngaard
72 and others, 2019; Zemp and others, 2009). They have been the subject of numerous glaciological studies
73 throughout the past decades, (e.g. Denzinger and others, 2021; Dirmhirn and Trojer, 1955; Etzelmüller
74 and others, 2000; Kuhn and others, 1999; Young, 1981). The availability of data and previous work to
75 understand these glaciers makes them ideal test sites for our novel approach.

76 **Hintereisferner**

77 Hintereisferner (46.798814°N 10.770068°E), located in the Ötztal Alps in Austria, is a clean-ice valley
78 glacier. Its 2011 area was approximately 6.78 km², about 15 % smaller than in 2001 (Klug and others,
79 2018). Its elevation ranges from 2238 m a.s.l. at the Little Ice Age (LIA) terminus, to about 3661 m
80 a.s.l. (Wijngaard and others, 2019). Meltwater from the Hintereisferner runs into the Hintereisbach, which
81 converges with runoff streams from nearby glaciers such as the Kesselwandferner. It finally drains into
82 the Ötztaler Ache, one of the main tributaries of the river Inn (Klug and others, 2018). The glacier is

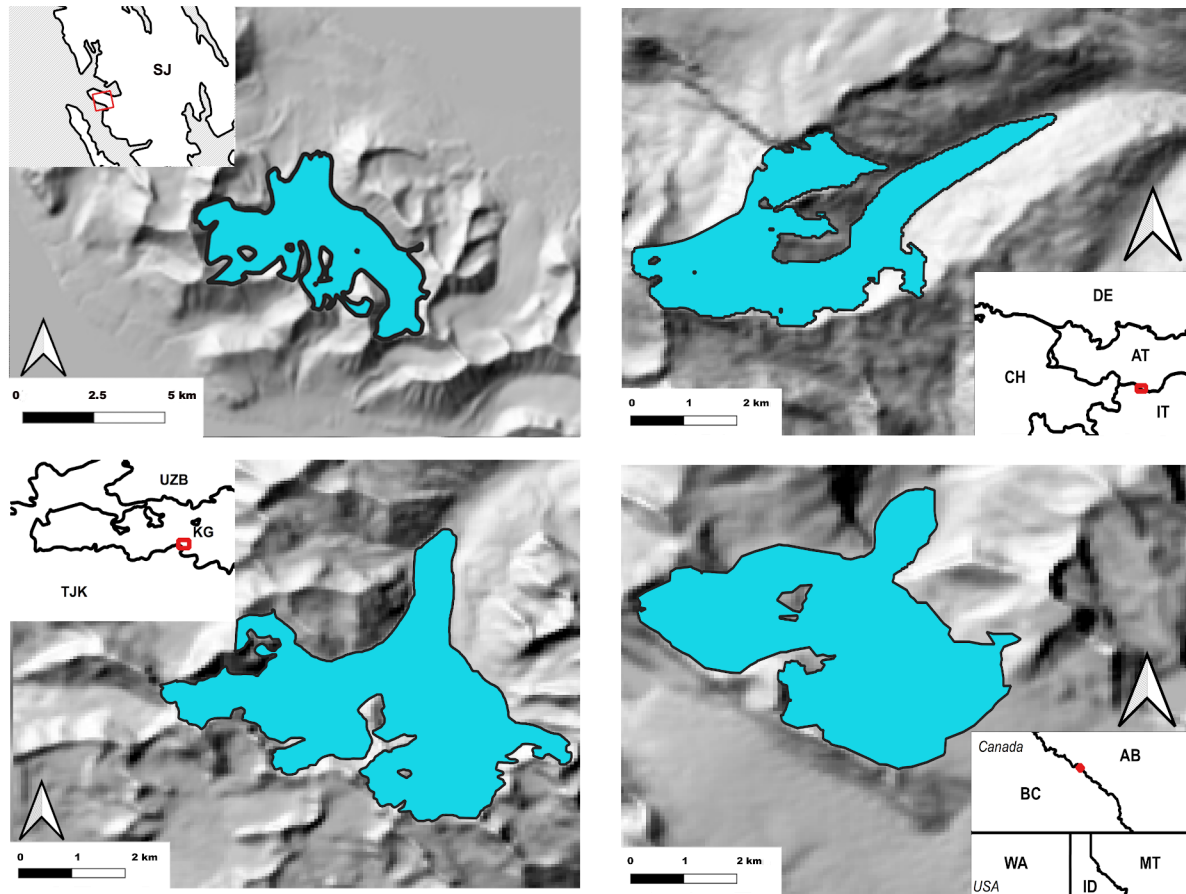


Fig. 1. Glacier outlines according to the (RGI Consortium, 2017), from top left in clockwise order: Austre Brøggerbreen (NO), Hintereisferner (AT), Peyto Glacier (CA) and Abramov Glacier (KGZ). Inset shows location of the map in their respective country, labels depicting state and/or country codes.

83 located in the "inner dry Alpine zone", one of the driest places in the European Alps. At the meteorological
84 station in Vent, located approximately 8 km West of the glacier, at 1900 m a.s.l., annual mean precipitation
85 is approximately 750 mm/a (1987-2016) and annual mean temperature is approximately 3°C (Klug and
86 others, 2018). Annual mean precipitation at the glacier is often up to double the amount of Vent (Fischer,
87 2013), confirmed by totalisator measurements, see Strasser and others (2018).

88 **Peyto Glacier**

89 Peyto glacier (51.678056°N, -116.547222°E) is a mountain glacier located in Banff National Park, Canada.
90 With its continued observation, Peyto glacier is considered an important "index glacier for the region"
91 (Kehrl and others, 2014). It had an area of 9.699 km² in 2006, and its elevation ranges from 2647 m a.s.l.
92 to 3032 m a.s.l. (Kehrl and others, 2014; Pradhananga and others, 2021). The glacier drains into Peyto
93 lake through Peyto Creek, which flows from a proglacial lake that has formed since 2002, and has been
94 informally named Lake Munro (Pradhananga and others, 2021). The glacier has continuously been losing
95 mass since at least the 1920s. It is located in a continental climatic regime, characterized by relatively
96 low precipitation inputs and large variability in temperature (Young, 1981). Temperature records from a
97 meteorological station on the glacier, set up by and available from (Pradhananga and others, 2021), show
98 that the daily average temperature varied between 15°C and -30°C during the period 2013-2018. Based on
99 records from the closes meteorological station at Bow Summit, approximately 15 km from the glacier, show
100 that total precipitation varies between 400 and 800 mm for winter (summed over 1 October - 31 March)
101 and between 200 and 500 mm for summer (summed over 1 April to 30 September) (Mukherjee and others,
102 2022).

103 **Austre Brøggerbreen**

104 Austre Brøggerbreen (78.89092°N, 11.84745°E) is a valley/ cirque glacier located on the archipelago of
105 Svalbard, Norway. It has an area of 6.12 km² (2012), and ranges in elevation from 50 to 650 m a.s.l. (RGI
106 Consortium, 2017; Bruland and Hagen, 2002). Like many glaciers on the archipelago, e.g. Longyearbreen
107 (78.1653°N, 15.4306°E), Austre Brøggerbreen has lost over 50% of its area since 1936. Austre Brøggerbreen
108 is situated in a High Arctic climate, characterized by low temperatures and relatively low precipitation,
109 though the meteorological stations in Longyearbyen and Ny-Ålesund, the latter approximately 4km from
110 the glacier, show the local climate to be comparatively warm to other locations between 70 and 80°N

111 (Eckerstorfer and Christiansen, 2011). The mean annual air temperature, measured at the equilibrium line
112 (approximately 300 m a.s.l.), is -8.0°C , while the mean annual temperature in Ny-Ålesund was -6.3°C in
113 the period 1969-1990, with an increase to -5.2°C from 1981-2010, due to arctic amplification (Førland and
114 others, 2011; López-Moreno and others, 2016). Mean annual precipitation in the area was 385 mm and
115 427 mm for the periods 1961-1990 and 1981-2010, respectively (Førland and others, 2011).

116 **Abramov Glacier**

117 The Abramov glacier (39.6022°N , 71.5508°E) is a valley glacier in the Koxsu Valley, Pamir-Alay range, in
118 Kyrgyzstan (Barandun and others, 2015). It has an area of 24 km^2 and spans an elevation range of 3650 to
119 5000 m a.s.l. (in 2015) (Kronenberg and others, 2021). Between 1975 and 2015, the glacier has lost about
120 5% of its area, and retreated approximately 1 km (Barandun and others, 2015). The Abramov glacier is
121 located in a continental climate. Mean annual temperature recorded at the glacier meteorological station
122 (3837 m a.s.l.) was -4.1°C for the period period 1968–1998 (Pertziger, 1996). Mean annual precipitation
123 was 750 mm from 1968-1998, with maximum precipitation occurring from March to May (Pertziger, 1996).

124 **DATA AND METHODS**

125 **The Open Global Glacier Model**

126 The Open Global Glacier Model (OGGM) is an open-source model framework for global past and future
127 glacier modelling developed by Maussion and others (2019). It is a modular framework with a glacier-centric
128 approach, of which we use only the mass balance model (v. 1.5.3) for the current study. The Randolph
129 Glacier Inventory (RGI) v. 6 forms the base of OGGM, while the digital elevation models (DEM) are
130 selected per glacier, from various available datasets in OGGM, depending on the region. For the current
131 study, the DEMs stem from NASADEM and COPDEM (Crippen and others, 2016; Fahrland and others,
132 2020, respectively). As needed, the model can also be operated on user-input DEM data.

133 These are then applied to each glacier outline. After the preprocessing, glacier centerlines are
134 computed, according to the Kienholz and others (2014) algorithm. These centerlines are then converted
135 into flowlines. For climate data, we timeseries of temperature and precipitation (TS: Harris and others,
136 2014) from the Climate Research Unit (CRU) dataset (Harris and others, 2014). These are then downscaled
137 to the CRU 1961-1990 CE climatology (New and others, 2002), by applying the 1961-1990 anomalies: a
138 robust statistical method, often referred to as the delta method or change factor method (e.g. Getahun

139 and others, 2021; Prudhomme and others, 2010). This is done in order to obtain time series with elevation
 140 data, which is not a feature of CRU TS. Temperature and precipitation are then applied in an extended
 141 'temperature index melt model', in which monthly mass balance is calculated according to:

$$m_i(z) = p_f P_i^{solid}(z) - \mu^* \max(T_i(z) - T_{melt}, 0), \quad (1)$$

142 in which $m_i(z)$ represents monthly mass balance at altitude z , P_i^{solid} is solid precipitation, calculated
 143 from the total monthly precipitation, according to a temperature threshold. In case monthly mean tem-
 144 perature $T_i(z)$ is below 0 °C all precipitation is considered solid; when the temperature is above 2 °C all
 145 precipitation is considered liquid. When the temperature is between these, the solid fraction decreases
 146 linearly. The default temperature lapse rate is set to 6.5 °C/km and the threshold temperature for melt to
 147 -1 °C. The precipitation correction factor p_f , that we apply to adjust precipitation in our scenario neutral
 148 approach (see Section Scenario-Neutral Approach), can generally be considered a correction for orographic
 149 precipitation, wind-blown snow and avalanches, when set to its default value of 2.5.

150 Finally, temperature sensitivity parameter μ^* comes from an automated calibration procedure. OGGM
 151 contains various modules to calibrate the mass balance model. Here μ^* is calibrated with observed WGMS
 152 mass balance data for the four glaciers in our case study. When modelling on a larger scale, the model can
 153 also be calibrated with all WGMS reference glaciers, geodetic mass balance data (e.g. Hugonnet and others,
 154 2021) or the user's own mass balance data. For more detailed information visit: <https://docs.oggm.org>
 155 and (Maussion and others, 2019).

156 CMIP6 Models

157 For the scenario projection approach, we force OGGM with temperature and precipitation from four
 158 GCMs, obtained from CMIP6 archived model output. These models are FGOALS3, MPI-ESM1, EG-
 159 Earth 3 and NorESM2. The specifications of each model are shown in Table 1, and we use the r1i1p1f1
 160 realization of all models. In order to obtain datasets spanning 2000-2100, we merge GCM output from
 161 the CMIP6 experiment 'historical', which spans the years 1850-2015, and GCM output under four SSPs
 162 (2015-2100): SSP 1-2.6, 2-4.5, 3-7.0 and 5-8.5 (O'Neill and others, 2016). These are driven by emissions and
 163 land-use scenarios and refer to climate mitigation, adaptation and impacts. SSP 1-2.6 (updated Relative
 164 Concentration Pathway 2.6 (RCP;(Van Vuuren and others, 2011)) refers to a level of radiative forcing of
 165 2.6 Wm⁻² in 2100 and represents the low end of the future forcing pathways. SSP 2-4.5 (updated RCP 4.5)

Table 1. CMIP6 GCMs applied in scenario projection approach

Model	Acronym	Components	Coupler
Version 3 of the Flexible Global Ocean Atmosphere Land System model (Li and others, 2020)	FGOALS 3	Version 3 of the Grid-Point Atmospheric Model of LASG-IAP (GAMIL3), Version 3 of the LASG-IAP Climate System Ocean Model (LICOM3), Version 4 of the Los Alamos sea ice model, the CAS-Land Surface Model (CAS-LSM)	Common Flux Coupler
Max Planck Institute Earth System Model (Müller and others, 2018)	MPI-ESM1	Atmospheric Model ECHAM6.3, Ocean Model MPIOM Version 1.6.2	Ocean-Atmosphere-Sea-Ice Coupler Version 4
EC-Earth 3 Earth System Model (Döscher and others, 2022)	EC-Earth3	Various Physical Domains and System Components describing Atmosphere, Ocean, Sea Ice, Land Surface, Dynamic Vegetation, Atmospheric Composition, Ocean Biogeochemistry and the Greenland Ice Sheet	OASIS3-MCT Coupling library
Version 2 of the Coupled Norwegian Earth System Model (Seland and others, 2020)	NorESM2	CIME: Configuration Handler, CAM6-Nor: Atmosphere and Aerosol, CICE5.1.2: Sea Ice, CLM5: Land and Vegetation, MOSART: River Transport, BLOM: Ocean, iHAMOCC: Ocean Carbon Cycle	CESM2 Coupler

166 refers to 4.5 Wm^{-2} as representing the medium level. SSP 3-7.0 is a newly added level at the high end of
 167 the range referring to 7 Wm^{-2} radiative forcing in 2100. SSP 5-8.5 (updated RCP 8.5), representing the
 168 high end of the future pathways, refers to 8.5 Wm^{-2} .

169 Comparison with Observed Data

170 In order to create a set of reference - unperturbed - results, we force the OGGM mass balance model
 171 with a baseline climate, from here on referred to as 'unperturbed'. These are the downscaled CRU time
 172 series of precipitation and temperature from 1985 until 2015. For the sake of simplicity, computational
 173 efficiency and consistency with the scenario-neutral method, we use fixed geometries throughout our model
 174 runs, corresponding to the outline at the glacier's RGI date. To ascertain that our baseline results are
 175 reliable, we compare the mass balance results of all four glaciers with the WGMS observed mass balance
 176 data (WGMS, 2022a), assessing skill via the calculation and analysis of the mass balance error (MBE),
 177 mean absolute error (MAE) and Pearson correlation. For the MBE, we subtract observed mass balance
 178 from modeled mass balance in the same year, for each glacier, over the period 1985-2015 (N=107, because
 179 of lack of observation for Abramov Glacier from 2000-2012). For the MAE, we take the absolute values of
 180 the 107 calculated MBEs, from which we calculate a mean MAE per glacier. The MAE, as it considers

181 the direction of error, provides more information about the magnitude of the discrepancy between modeled
182 and observed values. Finally, we calculate the Pearson correlation coefficient, as a a measure of agreement
183 between modeled and observed values.

184 **Scenario-Neutral Approach**

185 We define scenario-neutral as looking at the impact of changes in climate attributes, independently of each
186 other, of timing or other variables affecting the system. In our particular case, that means we analyze the
187 impact of changes in precipitation and temperature, relative to a baseline, in a multitude of combinations
188 (e.g. a 20% increase in precipitation and no change in temperature, a 10% decrease in precipitation
189 and 5°C increase in temperature, or both attributes remaining at baseline in summer, while changing in
190 winter), without these changes being associated with a particular climate change scenario. Scenario-neutral
191 methods look at system response, in this case the system 'glacier', where we define the response as a change
192 in climatic glacier mass balance. The magnitude of the response is a means to assess and convey system
193 sensitivity.

194 Because glacier mass balance is, in reality, also influenced by changes in glacier geometry, impacting
195 volume and area, we model mass balance using a fixed geometry. This allows us the advantage of modeling
196 glacier response to climate attribute changes under which the real-world glacier would have significantly
197 changed geometry or vanished entirely. The mass balance calculated from this diminishing volume and
198 area would be much lower, which would misrepresent the severity of the system response. Modeling glacier
199 mass balance with fixed geometries (here, the outline at their RGI date) allows comparison of sensitivity
200 on a glacier-to-glacier basis, regardless of their real-world mass loss over time, and is considered the more
201 climatically relevant type of mass balance (Elsberg and others, 2001).

202 Finally, in order to assess and convey system sensitivity at a glance, we make use of response surfaces.
203 These are two-dimensional, gridded plots, with each of the axes representing a climate attribute and the
204 system response depicted in a colour-coded grid.

205 For each of the four glaciers in our case study, we follow the steps towards construction of a scenario-
206 neutral space outlined in (Culley and others, 2021), which consist of the following:

207 **1) Selection of Climate Attributes:** As we consider four reference glaciers, whose mass balance is prin-
208 cipally governed by precipitation and temperature (Shea and Marshall, 2007; WGMS, 2022b), these
209 are the climate attributes against which we measure glacier response. These attributes form the axes

210 of our response surface, too. Our choice of climate attributes is also in line with the selection of
211 our system model for the calculation of system response: OGGM's mass balance model, which uses
212 monthly time series of precipitation and temperature as input.

213 **2) Development of Perturbed Attribute Values:** This considers the plausible changes in the selected
214 climate attributes. Since we consider the CMIP6 SSP scenarios, until 2100, within our response
215 surface boundaries, these give a guideline of the magnitude of our plausible changes. To calculate
216 upper boundaries for the perturbation, for mean annual temperature and annual precipitation, we
217 calculate the difference between the unperturbed mean values and SSP585 (most extreme) values
218 over the year 2100, for all four glaciers. The largest temperature difference is found for Austre
219 Brøggerbreen, with a mean annual temperature over the unperturbed period of -7.2°C and of 3.6°C
220 in 2100. To include this scenario in our boundaries, we apply a plausible perturbation of $+11^{\circ}\text{C}$.

221 For precipitation, in order to take into account the large differences in precipitation amount the
222 four glaciers get, we use a multiplicative factor rather than fixed amounts in- or decreased. Also
223 here, we find the largest differences from baseline in SSP585, and in this case for Hintereisferner
224 and Peyto glacier. For Hintereisferner, we see a decrease of 10%, from 1480 mm per year to 1330
225 mm per year between the unperturbed period and 2100. For Peyto glacier, we see an increase of
226 48% in precipitation, from 1148 mm per year to 1706 mm per year. To include these scenarios, we
227 include perturbations of -20% to +50% in precipitation. For the time slice 2010-2040, we adapted
228 the precipitation boundary for Austre Brøggerbreen to a decrease of 70%, to fit the CMIP6 scenarios
229 within the boundaries.

230 **3) Generation of Climate Perturbed Time Series:** To reflect these perturbations in our climate at-
231 tribute time series, we make use of a temperature bias and the precipitation factor (for the latter,
232 see Equation 1). The temperature bias simply adds a specified anomaly in $^{\circ}\text{C}$ to the unperturbed
233 time series, according to the increments of the response surface axes. Depending on the glacier, we
234 use increments of 0.5°C or 1°C . The precipitation factor is a multiplicative factor, which is calibrated
235 to 2.5 for our baseline climate. We adjust percentages according to our selected perturbations, in
236 increments of 5% to 10%, depending on the glacier. For the seasonality sensitivity experiments, either
237 winter (October-March) or summer (April-September) are kept constant, while the other season is
238 perturbed.

239 **4) Assessment of System Performance:** The system performance, here defined as climatic glacier
 240 mass balance, is calculated by forcing the OGGM mass balance model with each incrementally
 241 perturbed 30-year time series, for each glacier. The mean mass balance over the 30-year time period
 242 is calculated and depicted in the response surface grid.

243 **Glacier Sensitivity Index**

244 To quantify and support the visual impact of the response surface, we calculate the glacier sensitivity
 245 index (GSI), building upon the idea by Oerlemans and Reichert (2000) that mass balance can be related
 246 to precipitation and temperature with a sensitivity characteristic. The GSI is calculated per glacier, for
 247 temperature and precipitation. We only calculate the GSI in instances where the relevant climate attribute
 248 is perturbed, and the other is not, to isolate its impact. The calculation is done as follows:

$$GSI_T = (m_k - m_{ref,k})/bias_T, \quad (2)$$

249 and

$$GSI_P = (m_k - m_{ref,k})/factor_P, \quad (3)$$

250 in which m_k and $m_{ref,k}$ represent the mass balance in year k of the perturbed run, and year k of the
 251 unperturbed, baseline run. $Bias_T$ and $factor_P$ refer to the temperature bias and precipitation factor,
 252 respectively. GSI_T and GSI_P are calculated annually.

253 The magnitude and the inter-annual variability of the GSI values per climate attribute represent the
 254 influence of the specific attribute on mass balance, representing system response. The larger the GSI,
 255 the larger the influence of the attribute on the system. The larger the variability, the less consistent the
 256 influence of the climate attribute on the system.

257 **Scenario Projection Approach**

258 For the traditional, top-down, scenario projection approach, we force OGGM with the four CMIP6 SSP
 259 scenarios, as represented by four models, outlined in the Section CMIP6 Models. Here, too, we use a
 260 fixed geometry, starting from the year 2000, running to 2100. The projections are then superimposed onto
 261 the response surface. This is done by calculating the mean annual temperature and annual precipitation

Table 2. Statistics comparing observed and modeled mass balances from the OGGM unperturbed run, for all four glaciers. All values and standard deviations are mean values per glacier

Performance measure	Peyto Glacier	Hintereisferner	Austre Brøggerbreen	Abramov Glacier
MBE (m w.e.)	0.017 ± 0.60	-0.29 ± 0.51	-0.11 ± 0.36	0.057 ± 0.39
MAE (m w.e.)	0.47 ± 0.36	0.46 ± 0.35	0.31 ± 0.19	0.31 ± 0.23
Pearson correlation	0.50	0.80	0.40	0.73-0.11

262 over 30 years (2010-2040, 2040-2070 and 2070-2100) for each model and scenario (from here on 'model
 263 iteration'). The differences between these values and the unperturbed CRU values determine the position
 264 on the axes and thus on the response surface.

265 RESULTS

266 Unperturbed Run

267 For the period 1985-2015, we calculate the model performance measures outlined in Table 2. Both indi-
 268 vidually and averaged over all four glaciers, we see good agreement between modeled and observed mass
 269 balances. Averaged over all four glaciers, an MBE of -0.08 ± 0.46 m w.e. and MAE of 0.39 ± 0.28 m w.e.
 270 show that overall, the errors are small. They are comparable to the error values Eis and others (2021) found
 271 for the validation of their mass balance reconstruction over all reference glaciers. Figure 2 shows that the
 272 cumulative mass balances, observed and modeled, match well, though the model slightly underestimates
 273 the mass balance, for Hintereisferner and Austre Brøggerbreen in particular. For Abramov glacier, 13 of
 274 the 30 observed years are missing, so it is not possible to make a robust judgment of the goodness of fit in
 275 terms of cumulative mass balance over the whole period. This is why the years 2011-2015, though obser-
 276 vations exist, are removed from the figure. Overall, we are satisfied with the agreement between observed
 277 and modelled mass balance, and proceed with the results of this unperturbed run as the 'central square',
 278 at temperature bias=0 and precipitation factor=2.5 (standard parameter value).

279 Scenario-Neutral Approach

280 As outlined above, we generate response surfaces according to the four steps suggested in Culley and others
 281 (2021). Using the defined boundaries of plausible climate change, this results in a response surface over the
 282 period 1985-2015 for Peyto Glacier, Hintereisferner, Austre Brøggerbreen and Abramov Glacier, as shown

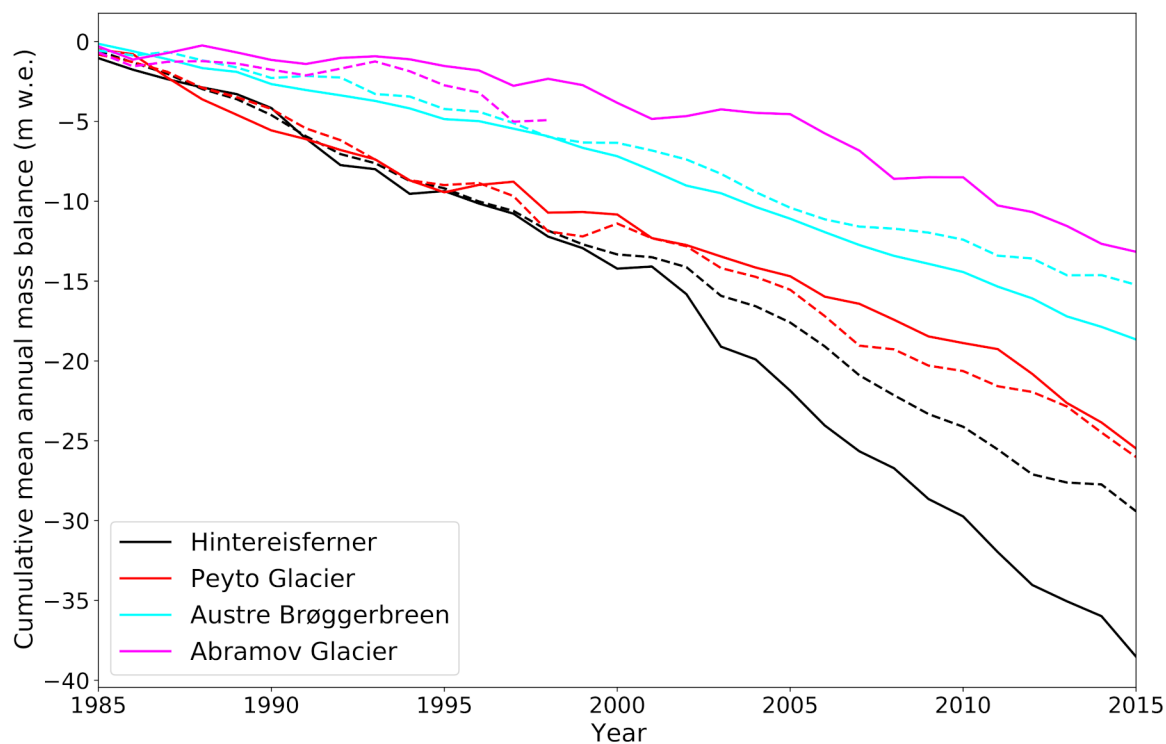


Fig. 2. Cumulative specific mass balance over the period 1985-2015, simulated with OGGM, forced with the unperturbed time series (solid lines), and observed (dashed lines) (WGMS, 2022a)

283 in figure 3. To assess the influence of seasonality of climate attributes on glacier mass balance, we also
284 generate a "known summer" and "known winter" response surface for each glacier, in which summer and
285 winter, respectively, are kept at their known values from the unperturbed run, and the respective other
286 season is perturbed. The results of this can be seen in figure 4.

287 Forced with the full unperturbed time series, Hintereisferner responds most sensitively to the changes
288 in climate attributes. Under the baseline, unperturbed climate, mean annual specific mass balance is -1.28
289 m w.e.. Under the most extreme scenario, with a decrease in precipitation of 20% and temperature increase
290 of 11°C, mean annual mass balance goes down to -22.55 m w.e.. Increases in precipitation markedly affect
291 mass balance in the realm of a temperature bias of -2°C to 2°C, after which precipitation ceases to have
292 an effect. This is likely due to a removal of accumulation from the mass balance equation (Equation 1)
293 entirely, as also winter temperatures are above the threshold at which precipitation falls as snow. For the
294 other glaciers, we see a less extreme response to the changes in climate attributes, though all glaciers follow
295 similar patterns, with an overall higher influence of temperature than precipitation. As Hintereisferner, out
296 of all glaciers show here, has the largest amount of annual precipitation, and the highest sensitivity, this
297 small case study confirms the ideas discussed in Meier (1984); Oerlemans and Fortuin (1992); Oerlemans
298 and Reichert (2000) that sensitivity goes up with precipitation amount, and that generally, glaciers with a
299 higher mass turnover are more sensitive to glaciers in climate.

300 Besides results for consistently perturbed time series, we also have response surfaces for seasonally
301 perturbed time series, depicted in figure 4. For clarity, we only discuss the two glaciers with the largest
302 differences in seasonal impact: Hintereisferner and Austre Brøggerbreen. The axes here have smaller
303 perturbations, in order to remain within the bounds of plausibility. The highest temperature bias is
304 of 3°C, which is in line with e.g. the exceptionally warm summer of 2022, in the Alps (Cremona and
305 others, 2022). These heat waves caused the mean annual temperature at the Hintereisferner station to
306 rise to -2.3°C at an altitude of 3245 m a.s.l. (Innsbruck University, 2022). The baseline climate mean
307 annual temperature, over 1985-2015, at Hintereisferner was -1.3°C at 2700 m a.s.l.. Adjusted for altitude,
308 using a lapse rate of 6.5°C/km, that would correspond to a temperature difference of 2.2°C, fitting within
309 perturbation limits.

310 As can be seen from the response surfaces in figure 4, there are marked differences in the responses of
311 Austre Brøggerbreen and Hintereisferner to seasonal perturbations. When the summer season is unper-
312 turbed, mass balance is only dependent on precipitation for Austre Brøggerbreen, while for Hintereisferner,

313 temperature remains influential. When winter is unperturbed, precipitation is of little importance for both
314 glaciers, and differences in mass balance are mostly due to temperature changes. The differing responses
315 of the glaciers are likely due to their location, and how much precipitation falls as snow. For Austre
316 Brøggerbreen, winter precipitation almost solely falls as snow. Perturbations within the boundaries shown
317 here would not affect this (figure 4 a). For Hintereisferner however, these increases in temperature would
318 affect the fraction of winter precipitation that falls as snow, impacting accumulation and thus mass balance
319 through both temperature and precipitation (figure 4 c). In summer, temperature changes mainly have an
320 effect on melt, and, of secondary importance, on the state of precipitation. For both glaciers, mass balance
321 almost exclusively changes with temperature, affecting the amount of melt. Precipitation has little to no
322 influence, likely due to little of summer precipitation falling as snow at these temperatures. The results
323 discussed here are in line with Oerlemans and Reichert (2000), who observe similar results when comparing
324 Nigardsbreen (Norway) and Franz-Josef glacier (New Zealand), which have comparable differences in their
325 precipitation patterns. Oerlemans and Reichert (2000) do note the importance of Hintereisferner summer
326 precipitation for its mass balance, which we do not observe in our response surfaces.

327 **Glacier sensitivity index**

328 The GSI results overlap with and complement the visual results in the response surfaces. For Hintereis-
329 ferner, GSI_T varies between $1.12 \text{ m w.e. } ^\circ\text{C}^{-1}$ and $1.96 \text{ m w.e. } ^\circ\text{C}^{-1}$, while for Austre Brøggerbreen, GSI_T
330 varies between $0.32 \text{ m w.e. } ^\circ\text{C}^{-1}$ and $0.56 \text{ m w.e. } ^\circ\text{C}^{-1}$. For Peyto and Abramov glacier respectively,
331 GSI_T values vary between $0.56 \text{ m w.e. } ^\circ\text{C}^{-1}$ and $0.81 \text{ m w.e. } ^\circ\text{C}^{-1}$, and $0.41 \text{ w.e. } ^\circ\text{C}^{-1}$ and 0.62 m w.e.
332 $^\circ\text{C}^{-1}$. The magnitude indicates the largest influence of temperature on mass balance for Hintereisferner,
333 as is also visible in figure 3.

334 For precipitation, the influence is more difficult to quantify in a sensitivity characteristic, because it
335 is very dependent on the temperature whether precipitation affects mass balance. At low temperatures,
336 when precipitation falls as snow and adds to accumulation, the amount of annual precipitation matters.
337 As an example, for Hintereisferner, GSI_P ranges between -0.8 m w.e. and 2.1 m w.e. at temperature bias
338 ranges -2 to 3°C . At higher temperature biases, GSI_P reaches values as low as -22.2 m w.e. . For Austre
339 Brøggerbreen, these ranges lie between -0.7 and 0.6 m w.e. at temperature bias -2 to 3°C , and go up
340 to -4.11 m w.e. at a temperature bias of 11°C . This is consistent with the visual results of the response
341 surfaces, where mass balance varies with precipitation in the left columns, at lower temperature biases,

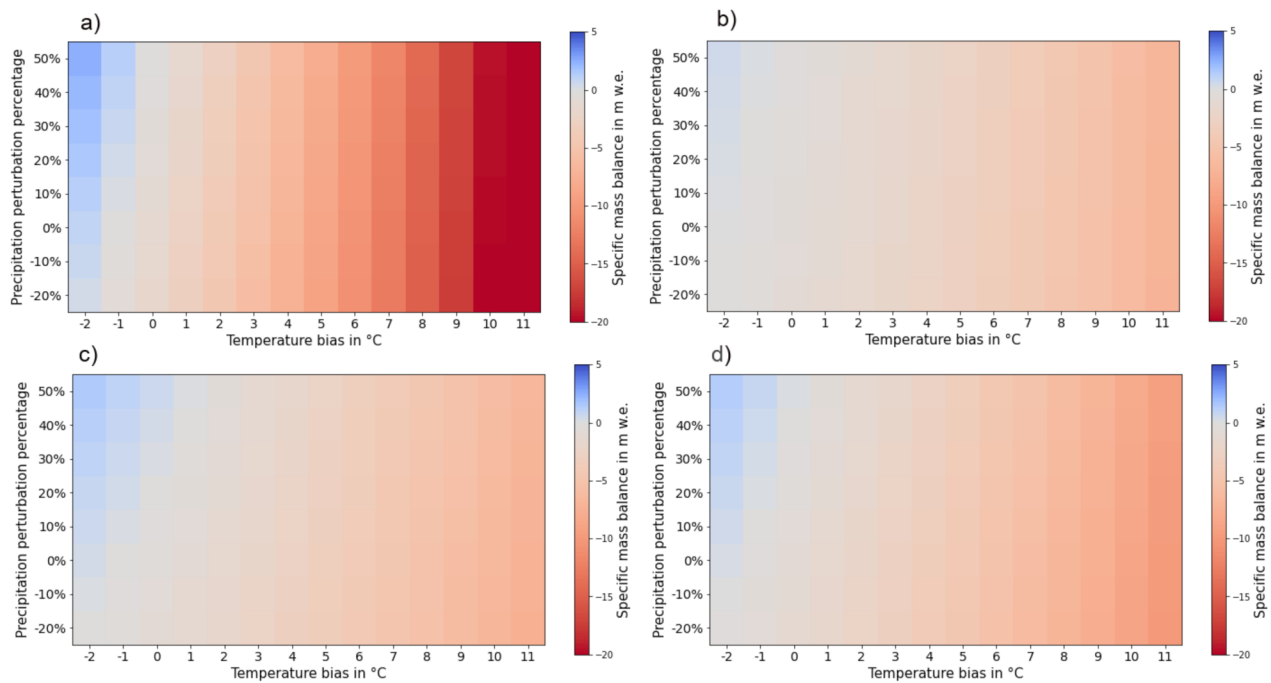


Fig. 3. Response surfaces for a) Hintereisferner, b) Austre Brøggerbreen, c) Abramov Glacier and d) Peyto Glacier, resulting from the fully perturbed time period 1985-2015. Mass balance values represent the annual mean over the 30-year time period. For comparison purposes, the color bars are unified and the transition blue-orange is centered at 0 m w.e.

342 and remains more consistent as the temperature bias increases.

343 Scenario projections

344 For all four glacier, we calculate the development of their mass balance under the four SSPs, with the
 345 models described in Section CMIP6 Models. The results are superimposed onto the response surfaces,
 346 as a means to estimate the impact of the given climate change projection, as also seen in e.g. Kay and
 347 others (2014) and Culley and others (2021). First, two example results are given here, in figure 5, for
 348 glaciers Austre Brøggerbreen and Hintereisferner, and time slice 2070-2100. On the response surface, we
 349 observe clear differences between the different models in their manifestation of the SSPs. For both glaciers,
 350 EC-Earth 3 has the largest increase in temperature and precipitation from the baseline climate, while
 351 FGOALS 3 projects the lowest increases in temperature, and a decrease in precipitation rather than an
 352 increase. NorESM2 and MPI-ESM1 show similar responses, with little change in precipitation. For Austre
 353 Brøggerbreen, we see that the EC-Earth 3 SSP126 scenario indicates a larger increase in temperature than

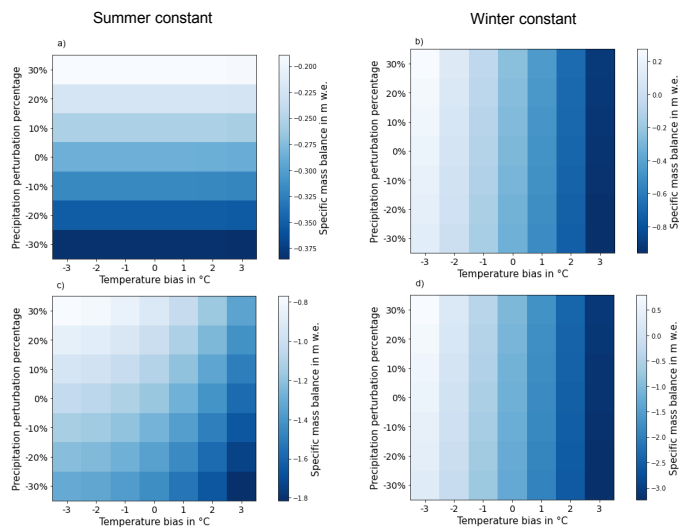


Fig. 4. Response surfaces for Austre Brøggerbreen (a and b) and Hintereisferner (c and d), resulting from the seasonally perturbed time period 1985-2015. The word 'constant' at top of the figure refers to a perturbation of 0 for that season in all years. Mass balance values represent the annual mean over the 30-year time period. The summer contribution to mass balance for 'summer constant' is -1.07 m w.e. for Austre Brøggerbreen (a) and -3.84 m w.e. for Hintereisferner (c). For 'winter constant', the winter contributions to mass balance are 0.49 m w.e. (b) and 1.49 m w.e. (d). For clear contrast of the colors, and thus of the differences per season and glacier, the color scales are not unified, so please note.

354 all, more extreme, SSPs in the other models. This shows the high potential uncertainty in the use of
355 climate change projections, when applied to glacier mass balance.

356 Because of the realization that by 2070-2100, the present-day geometry used in our OGGM runs would
357 no longer be representative of the glacier state, we present a more zoomed-in response surface in figure
358 6. Overlaid here are the SSPs as represented by the four GCMS, for the time period 2010-2040. As the
359 differences between the baseline climate and SSP climates are smaller here for temperature, but larger for
360 precipitation, the axes are adapted to focus on this range. We see that over this period, the projections
361 have diverged much less than for 2070-2100, but the differences between models remain.

362 DISCUSSION

363 The methods applied here depart from the conventionally used top-down approach of modelling glacier
364 response to pre-defined climate change scenarios. The aim was to apply a scenario-neutral approach
365 in glaciology, expanding their use to this research field. We endeavor to show the overall and seasonal
366 sensitivity of four different glaciers to changes in precipitation and temperature, as well as use this approach
367 as a framework in which to analyze pre-defined climate change scenarios. Especially the simplicity and
368 two-folded type of result - visually in response surfaces and quantified in the GSI - form the method's
369 strength. However, there are significant limitations as well, pertaining to the use of a fixed geometry, only
370 four glaciers, and the generation of the perturbed time series.

371 Sensitivity

372 Overall, the use of this scenario neutral approach can provide a comprehensive overview of a glacier's
373 sensitivity to temperature and precipitation. As we see above, the response surfaces clearly exhibit the
374 high sensitivity of the Hintereisferner, especially to temperature changes, compared to the other three
375 glaciers in our study. The same is conveyed through the Hintereisferner having the highest GSI_T (1.12 m
376 w.e./°C - 1.96 m w.e./°C). The numbers for the GSI_T are in line with the observed temperature sensitivity
377 for the glacier calculated by Fischer (2010) after 1979, which ranges between 0.38 m w.e./°C and 1.54 mm
378 w.e./°C.

379 This type of sensitivity analysis is more difficult to reach through the use of top-down methods with
380 scenario projections, as they are highly uncertain and do not cover the total range of plausible changes in
381 climate, especially on smaller scales, such as the glacier or basin scale. Neither are pre-defined projections

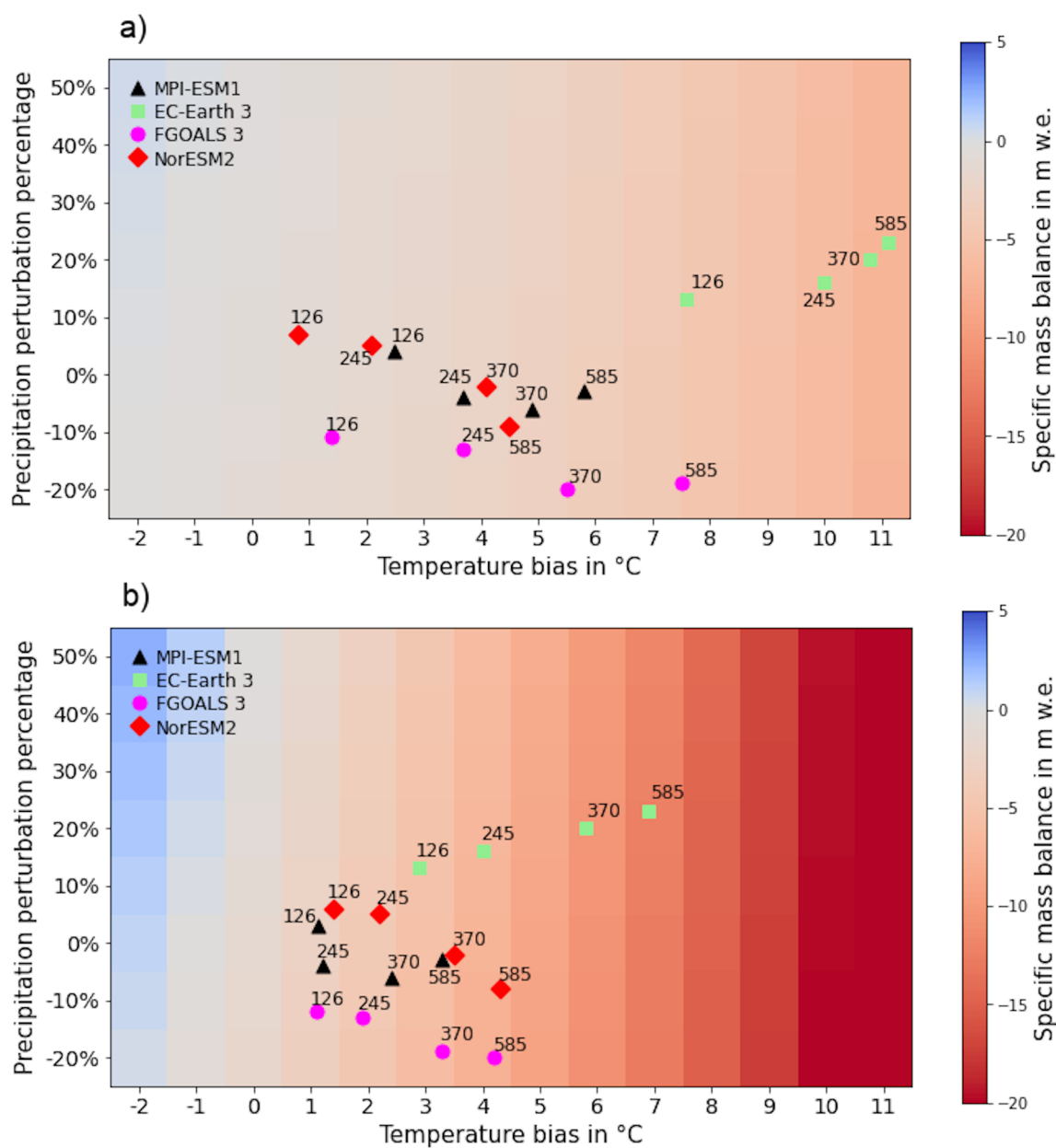


Fig. 5. Response surfaces for Austre Brøggerbreen (a) and Hintereisferner (b), with the SSPs for all models overlaid, averaged over the period 2070-2100

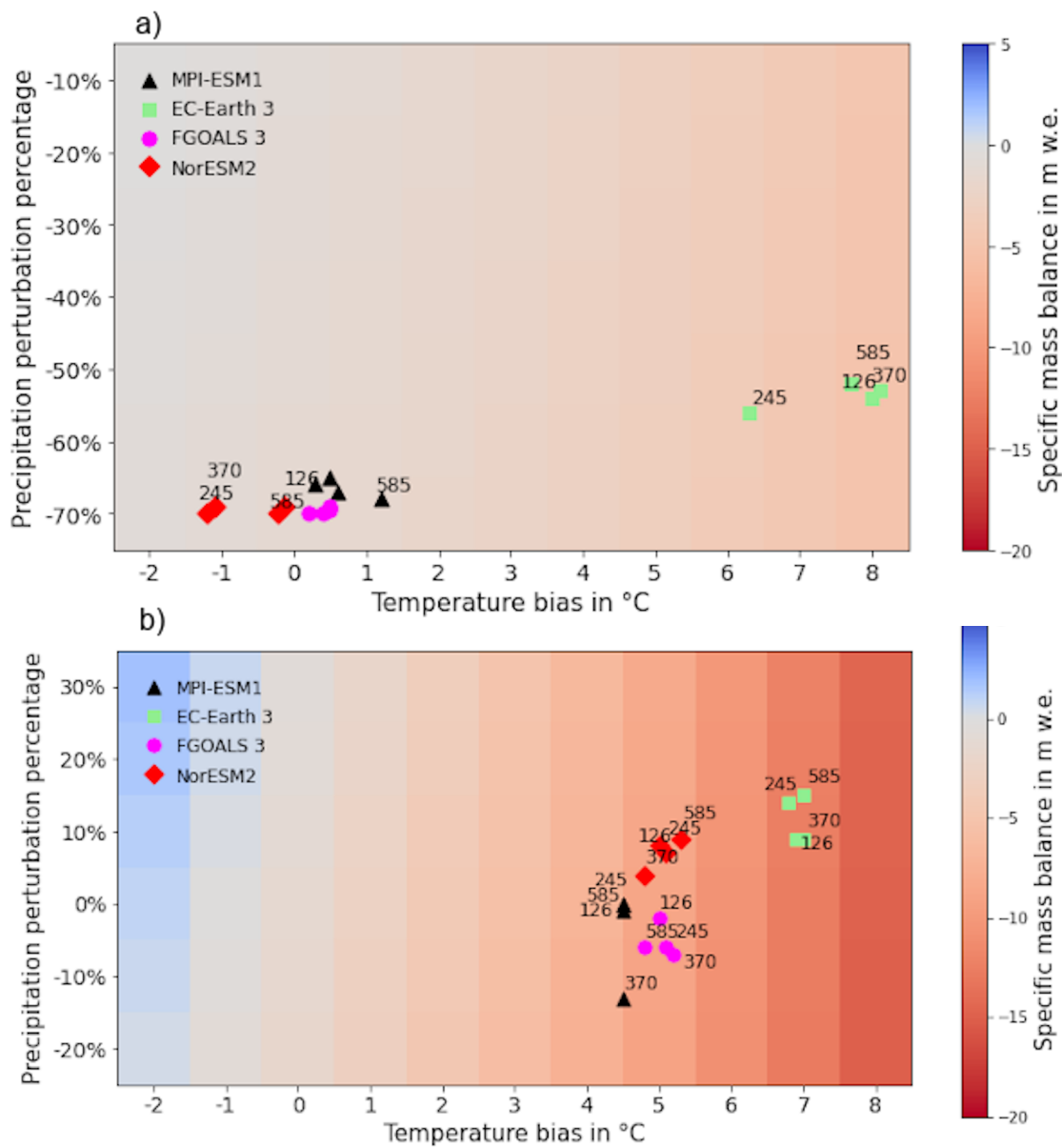


Fig. 6. Response surfaces for Austre Brøggerbreen (a) and Hintereisferner (b), with the SSPs for all models overlaid, averaged over the period 2010-2040. Note the difference in precipitation axes for the two glaciers. For Austre Brøggerbreen, the differences between several SSPs for models MPI-ESM1 and FGOALS 3 are so small that they are not labeled, for legibility purposes

382 well suited for direct glacier comparison, as the changes in climate differ per glacier. Through response
383 surfaces and *GSI*, glacier response to the same range of plausible changes in temperature and precipitation
384 can be compared in a computationally inexpensive way.

385 **Seasonal response**

386 In terms of seasonal sensitivity, the scenario neutral approach is especially useful in determining the impact
387 of climate characteristics per season. By keeping one season unperturbed, the impact of perturbations in
388 the other can be isolated. By keeping perturbation ranges the same, comparisons of responses can be made
389 between glaciers. As done here, for two glaciers, it provides insight into the differing importance of single
390 seasons and climate characteristics per glacier. This knowledge can be applied to uncertainty analysis
391 in studies of these glaciers, and judging the importance of said uncertainties, in discussing reliability of
392 observation or model results.

393 A limitation here is that of course, climate change is not limited to one season only, and the resulting
394 mass balances cannot be taken as true results for seasonal climate change perturbations. However, when a
395 season is known through observations, such as precipitation and temperature from glacier weather stations,
396 response surfaces can be used to provide the likely boundaries of the annual balance. As continuous mass
397 balance observations are only available for very few glaciers (Landmann and others, 2021), these boundaries
398 can provide an intermediate step of knowledge, before annual mass balance is observed or modelled. The
399 model would be forced with the known winter season values, an average of previous summer values, and
400 plausible summer perturbations. Especially if the known season is out of the ordinary, e.g. especially
401 dry, this can provide valuable knowledge for the annual mass balance range to follow. One example of this
402 could be for the current winter, 2022-2023, the first three months of which are strongly below the 2012-2022
403 accumulation average for Swiss glaciers (Switzerland, 2022).

404 **Scenario projections**

405 The main goal of superimposing scenario projections onto the scenario-neutral response surfaces is to gauge
406 their time line and the differences between projections and models. In the examples here, they provide
407 clear indications of model differences and ranges of glacier response. Especially on shorter time scales,
408 such as the decadal scale, where fixed geometry mass balance still matches observed balances well (van der
409 Laan and others, 2022), these overlays can provide a useful first step for dynamical modelling studies, as

410 they can be done before running the impact model. This type of rapid assessment is generally considered
411 the greatest asset of scenario neutral approaches in climate change studies (Prudhomme and others, 2010;
412 Kay and others, 2014)

413 **Limitations and outlook**

414 Finally, while scenario neutral approaches can be useful, there are important limitations to the interpreta-
415 tion of their results, especially considering we only study four glaciers here. The most limiting factor here,
416 for both the *GSI* and response surfaces from this study, is the difference between mass balance response
417 here, and mass balance response in reality, the latter under changing glacier geometry. Especially on larger
418 time scales, mass balances under severe changes in climate will develop in line with both climate and the
419 glacier's changes in area, volume and altitude. That is why the response surfaces here cannot be interpreted
420 as the full, true glacier response to climate change. If a scenario neutral approach were to be applied in
421 dynamical glacier modelling, other response variables than mass balance become available: volume, area
422 and runoff. Two consistent response variables would be volume and area, rather than runoff, as the latter
423 two is subject to a peak, referred to as peak water, and then decreases as the glacier shrinks (Förster and
424 van der Laan, 2022; Huss and Hock, 2018). This feature could also be utilized, identifying under which
425 different combinations of temperature and precipitation perturbation peak water would arise. The overlay-
426 ing of scenario projection time slices then gives information on timing of these peak water conditions, and
427 with that give a critical system threshold for communities downstream. This would be one way of making
428 scenario neutral approaches useful for management purposes, as is already the case for flood management
429 (Kay and others, 2014).

430 The outlook for future application of scenario neutral approaches in OGGM could lie in running the
431 dynamical model, but the main priority of this method will lie in sensitivity studies, rapid comparison of
432 glaciers and educational purposes. The latter will mainly be done in the interactive module of OGGM Edu
433 (OGGM, 2022), an educational platform by the OGGM consortium (Maussion and others, 2019). Through
434 the response surfaces, glacier sensitivity to climate change can be illustrated, in addition to OGGM Edu
435 applications such as the mass balance simulator. The method can easily be extended from the four glaciers
436 presented here, to all land-terminating glaciers listed in the RGI, which should be done as a pilot with all
437 279 land-terminating reference glaciers, before implementing this on a larger scale.

438 CONCLUSION

439 Overall, we conclude that scenario neutral approaches are very suitable to the modelling of glacier mass
440 balance, due to precipitation and temperature being its main drivers. The method yields visual output
441 that is easily understood, also by non-experts in the field of glaciology, and a quantification in the form
442 of the *GSI*. Both these results make it easy to rapidly compare the sensitivity of glaciers to changes in
443 climate, as well as the seasonal importance of precipitation and temperature. The method confirming long-
444 standing ideas in glaciology, such as the relationship between sensitivity and precipitation and temperature
445 (Meier, 1984; Oerlemans and Fortuin, 1992), shows consistency, while adding new features, such as response
446 surfaces providing boundaries to a range of future mass balances. This can be especially valuable when
447 only one season is known. Overlaying scenario projections can also deliver an additional step of knowledge,
448 in which the response surface becomes the framework in which to compare time lines of projections and
449 differences between models and scenarios. While there are limits to their interpretation, mainly due to
450 using a fixed geometry in this study, scenario neutral approaches are an additional, easy, and useful facet
451 to sensitivity studies in particular, and mass balance modelling studies as a whole.

452 [Scenario-neutral Mass Balance Modelling]A scenario-Neutral Approach to Climate Change in Glacier
453 Mass Balance Modelling [van der Laan]Larissa van der Laan, Kim Cholibois, Ayscha El Menuawy and
454 Kristian Förster

455 ACKNOWLEDGEMENTS

456 We would like to thank Lizz Ultee for her advice, motivating words and helpful discussions regarding
457 this project. Thanks also goes out to Fabien Maussion, for building the OGGM community and his
458 constructive comments that helped this research underway. This project was funded by the German
459 Research Foundation, Project GLISSADE, no. 416069075

460 REFERENCES

- 461 Barandun M, Huss M, Sold L, Farinotti D, Azisov E, Salzmann N, Usubaliev R, Merkushkin A and Hoelzle M (2015)
462 Re-analysis of seasonal mass balance at abramov glacier 1968–2014. *Journal of Glaciology*, **61**(230), 1103–1117
- 463 Beylich M, Haberlandt U and Reinstorf F (2021) Daily vs. hourly simulation for estimating future flood peaks in
464 mesoscale catchments. *Hydrology Research*, **52**(4), 821–833

- 465 Brighenti S, Tolotti M, Bruno MC, Wharton G, Pusch MT and Bertoldi W (2019) Ecosystem shifts in alpine streams
466 under glacier retreat and rock glacier thaw: A review. *Science of the Total Environment*, **675**, 542–559
- 467 Bruland O and Hagen JO (2002) Glacial mass balance of austre brøggerbreen (spitsbergen), 1971–1999, modelled
468 with a precipitation-run-off model. *Polar Research*, **21**(1), 109–121
- 469 Cremona A, Huss M, Landmann J, Borner J and Farinotti D (2022) Heat wave contribution to 2022's extreme glacier
470 melt from automated real-time ice ablation readings. *The Cryosphere Discussions*, 1–27
- 471 Crippen R, Buckley S, Belz E, Gurrola E, Hensley S, Kobrick M, Lavallo M, Martin J, Neumann M, Nguyen Q and
472 others (2016) Nasadem global elevation model: Methods and progress
- 473 Culley S, Maier HR, Westra S and Bennett B (2021) Identifying critical climate conditions for use in scenario-neutral
474 climate impact assessments. *Environmental Modelling & Software*, **136**, 104948
- 475 Denzinger F, Machguth H, Barandun M, Berthier E, Girod L, Kronenberg M, Usubaliev R and Hoelzle M (2021)
476 Geodetic mass balance of abramov glacier from 1975 to 2015. *Journal of Glaciology*, **67**(262), 331–342
- 477 Dirmhirn I and Trojer E (1955) Albedountersuchungen auf dem hintereisferner. *Archiv für Meteorologie, Geophysik
478 und Bioklimatologie, Serie B*, **6**(4), 400–416
- 479 Döscher R, Acosta M, Alessandri A, Anthoni P, Arsouze T, Bergman T, Bernardello R, Boussetta S, Caron LP,
480 Carver G, Castrillo M, Catalano F, Cvijanovic I, Davini P, Dekker E, Doblas-Reyes FJ, Docquier D, Echevarria
481 P, Fladrich U, Fuentes-Franco R, Gröger M, v Hardenberg J, Hieronymus J, Karami MP, Keskinen JP, Koenigk
482 T, Makkonen R, Massonnet F, Ménégos M, Miller PA, Moreno-Chamarro E, Nieradzik L, van Noije T, Nolan P,
483 O'Donnell D, Ollinaho P, van den Oord G, Ortega P, Prims OT, Ramos A, Reerink T, Rousset C, Ruprich-Robert
484 Y, Le Sager P, Schmith T, Schrödner R, Serva F, Sicardi V, Sloth Madsen M, Smith B, Tian T, Tourigny E, Uotila
485 P, Vancoppenolle M, Wang S, Wårlind D, Willén U, Wyser K, Yang S, Yepes-Arbós X and Zhang Q (2022) The
486 ec-earth3 earth system model for the coupled model intercomparison project 6. *Geoscientific Model Development*,
487 **15**(7), 2973–3020 (doi: 10.5194/gmd-15-2973-2022)
- 488 Eckerstorfer M and Christiansen HH (2011) The “high arctic maritime snow climate” in central svalbard. *Arctic,
489 Antarctic, and Alpine Research*, **43**(1), 11–21
- 490 Eis J, Van der Laan L, Maussion F and Marzeion B (2021) Reconstruction of past glacier changes with an ice-flow
491 glacier model: Proof of concept and validation. *Frontiers in Earth Science*, **9**, 595755
- 492 Elsberg D, Harrison W, Echelmeyer K and Krimmel R (2001) Quantifying the effects of climate and surface change
493 on glacier mass balance. *Journal of Glaciology*, **47**(159), 649–658

- 494 Etzelmüller B, Ødegård RS, Vatne G, Mysterud RS, Tønning T and Sollid JL (2000) Glacier characteristics and
495 sediment transfer system of longyearbreen and larsbreen, western spitsbergen. *Norsk Geografisk Tidsskrift*, **54**(4),
496 157–168
- 497 Fahrland E, Jacob P, Schrader H, and Kahabka H (2020) Copernicus dem: Copernicus digital elevation model
498 product handbook. *Report AO/1-9422/18/IL G*
- 499 Farinotti D, Round V, Huss M, Compagno L and Zekollari H (2019) Large hydropower and water-storage potential
500 in future glacier-free basins. *Nature*, **575**(7782), 341–344
- 501 Fischer A (2010) Glaciers and climate change: Interpretation of 50 years of direct mass balance of hintereisferner.
502 *Global and Planetary Change*, **71**(1-2), 13–26
- 503 Fischer A (2013) Long-term glacier monitoring at the lter test sites hintereisferner, kesselwandferner and jamtalferner
504 and other glaciers in tyrol: a source of ancillary information for biological succession studies. *Plant ecology &*
505 *diversity*, **6**(3-4), 537–547
- 506 Førland EJ, Benestad R, Hanssen-Bauer I, Haugen JE and Skaugen TE (2011) Temperature and precipitation
507 development at svalbard 1900–2100. *Advances in Meteorology*, **2011**
- 508 Förster K and van der Laan LN (2022) A review on observed historical changes in hydroclimatic extreme events over
509 europe. *Climate Impacts on Extreme Weather*, 131–144
- 510 Frederikse T, Landerer F, Caron L, Adhikari S, Parkes D, Humphrey VW, Dangendorf S, Hogarth P, Zanna L, Cheng
511 L and others (2020) The causes of sea-level rise since 1900. *Nature*, **584**(7821), 393–397
- 512 Getahun GW, Zewdu EA and Mekuria AD (2021) Statistical downscaling (delta method) of precipitation and tem-
513 perature for bilate watershed, ethiopia. *International Journal of Water Resources and Environmental Engineering*,
514 **13**(1), 20–29
- 515 Guo D, Westra S and Maier HR (2017) Use of a scenario-neutral approach to identify the key hydro-meteorological
516 attributes that impact runoff from a natural catchment. *Journal of hydrology*, **554**, 317–330
- 517 Guo D, Westra S and Maier HR (2018) An inverse approach to perturb historical rainfall data for scenario-neutral
518 climate impact studies. *Journal of hydrology*, **556**, 877–890
- 519 Harris I, Jones P, Osborn T and Lister D (2014) Updated high-resolution grids of monthly climatic observations—the
520 CRU TS3.10 Dataset. *International Journal of Climatology*, **34**(3), 623–642 (doi: 10.1002/joc.3711)
- 521 Hinkel J, Church JA, Gregory JM, Lambert E, Le Cozannet G, Lowe J, McInnes KL, Nicholls RJ, van der Pol TD
522 and van de Wal R (2019) Meeting user needs for sea level rise information: a decision analysis perspective. *Earth's*
523 *Future*, **7**(3), 320–337

- 524 Hock R, Bliss A, Marzeion B, Giesen RH, Hirabayashi Y, Huss M, Radić V and Slangen AB (2019) Glaciernip-a
525 model intercomparison of global-scale glacier mass-balance models and projections. *Journal of Glaciology*, **65**(251),
526 453–467
- 527 Hugonnet R, McNabb R, Berthier E, Menounos B, Nuth C, Girod L, Farinotti D, Huss M, Dussailant I, Brun F and
528 others (2021) Accelerated global glacier mass loss in the early twenty-first century. *Nature*, **592**(7856), 726–731
- 529 Huss M and Hock R (2018) Global-scale hydrological response to future glacier mass loss. *Nature Climate Change*,
530 **8**(2), 135–140
- 531 Innsbruck University A (2022) Temperature data hintereis 1. [https://www.foto-webcam.eu/webcam/
532 hintereisferner1/](https://www.foto-webcam.eu/webcam/hintereisferner1/), accessed: 2022-12-20
- 533 Jansson P, Hock R and Schneider T (2003) The concept of glacier storage: a review. *Journal of Hydrology*, **282**(1-4),
534 116–129
- 535 Kay A, Crooks S and Reynard N (2014) Using response surfaces to estimate impacts of climate change on flood
536 peaks: assessment of uncertainty. *Hydrological Processes*, **28**(20), 5273–5287
- 537 Kehrl LM, Hawley RL, Osterberg EC, Winski DA and Lee AP (2014) Volume loss from lower peyto glacier, alberta,
538 canada, between 1966 and 2010. *Journal of Glaciology*, **60**(219), 51–56
- 539 Keller L, Rössler O, Martius O and Weingartner R (2019) Comparison of scenario-neutral approaches for estimation
540 of climate change impacts on flood characteristics. *Hydrological Processes*, **33**(4), 535–550
- 541 Kemp L, Xu C, Depledge J, Ebi KL, Gibbins G, Kohler TA, Rockström J, Scheffer M, Schellnhuber HJ, Steffen W
542 and others (2022) Climate endgame: Exploring catastrophic climate change scenarios. *Proceedings of the National
543 Academy of Sciences*, **119**(34), e2108146119
- 544 Kienholz C, Rich JL, Arendt AA and Hock R (2014) A new method for deriving glacier centerlines applied to glaciers
545 in alaska and northwest canada. *The Cryosphere*, **8**(2), 503–519 (doi: 10.5194/tc-8-503-2014)
- 546 Klug C, Bollmann E, Galos SP, Nicholson L, Prinz R, Rieg L, Sailer R, Stötter J and Kaser G (2018) Geodetic
547 reanalysis of annual glaciological mass balances (2001–2011) of hintereisferner, austria. *The Cryosphere*, **12**(3),
548 833–849
- 549 Kronenberg M, Machguth H, Eichler A, Schwikowski M and Hoelzle M (2021) Comparison of historical and recent
550 accumulation rates on abramov glacier, pamir alay. *Journal of Glaciology*, **67**(262), 253–268
- 551 Kuhn M, Dreiseitl E, Hofinger S, Markl G, Span N and Kaser G (1999) Measurements and models of the mass
552 balance of hintereisferner. *Geografiska Annaler: Series A, Physical Geography*, **81**(4), 659–670

- 553 Landmann JM, Künsch HR, Huss M, Ogier C, Kalisch M and Farinotti D (2021) Assimilating near-real-time mass
554 balance stake readings into a model ensemble using a particle filter. *The Cryosphere*, **15**(11), 5017–5040
- 555 Li L, Yu Y, Tang Y, Lin P, Xie J, Song M, Dong L, Zhou T, Liu L, Wang L, Pu Y, Chen X, Chen L, Xie Z, Liu
556 H, Zhang L, Huang X, Feng T, Zheng W, Xia K, Liu H, Liu J, Wang Y, Wang L, Jia B, Xie F, Wang B, Zhao
557 S, Yu Z, Zhao B and Wei J (2020) The flexible global ocean-atmosphere-land system model grid-point version 3
558 (fgoals-g3): Description and evaluation. *Journal of Advances in Modeling Earth Systems*, **12**(9), e2019MS002012
559 (doi: <https://doi.org/10.1029/2019MS002012>)
- 560 López-Moreno J, Boike J, Sanchez-Lorenzo A and Pomeroy J (2016) Impact of climate warming on snow processes
561 in ny-ålesund, a polar maritime site at svalbard. *Global and Planetary Change*, **146**, 10–21
- 562 Marzeion B, Champollion N, Haeberli W, Langley K, Leclercq P and Paul F (2017) Observation-based estimates of
563 global glacier mass change and its contribution to sea-level change. *Integrative study of the mean sea level and its
564 components*, 107–132
- 565 Marzeion B, Hock R, Anderson B, Bliss A, Champollion N, Fujita K, Huss M, Immerzeel WW, Kraaijenbrink P,
566 Malles JH and others (2020) Partitioning the uncertainty of ensemble projections of global glacier mass change.
567 *Earth's Future*, **8**(7), e2019EF001470
- 568 Maussion F, Butenko A, Champollion N, Dusch M, Julia Eis KF, Gregor P, Jarosch AH, Landmann J, Oesterle F,
569 Recinos B, Rothenpieler T, Vlug A, Wild CT and Marzeion B (2019) The Open Global Glacier Model (OGGM)
570 v1.1. *Geoscientific Model Development*, **2019**, 909–931 (doi: [10.5194/gmd-12-909-2019](https://doi.org/10.5194/gmd-12-909-2019))
- 571 Meier MF (1984) Contribution of small glaciers to global sea level. *Science*, **226**(4681), 1418–1421
- 572 Milner AM, Khamis K, Battin TJ, Brittain JE, Barrand NE, Füreder L, Cauvy-Fraunié S, Gíslason GM, Jacobsen
573 D, Hannah DM and others (2017) Glacier shrinkage driving global changes in downstream systems. *Proceedings
574 of the National Academy of Sciences*, **114**(37), 9770–9778
- 575 Mukherjee K, Menounos B, Shea J, Morteza pour M, Ednie M and Demuth MN (2022) Evaluation of surface mass-
576 balance records using geodetic data and physically-based modelling, place and peyto glaciers, western canada.
577 *Journal of Glaciology*, 1–18
- 578 Müller WA, Jungclaus JH, Mauritsen T, Baehr J, Bittner M, Budich R, Bunzel F, Esch M, Ghosh R, Haak H, Ilyina
579 T, Kleine T, Kornbluh L, Li H, Modali K, Notz D, Pohlmann H, Roeckner E, Stemmler I, Tian F and Marotzke
580 J (2018) A higher-resolution version of the max planck institute earth system model (mpi-esm1.2-hr). *Journal of
581 Advances in Modeling Earth Systems*, **10**(7), 1383–1413 (doi: <https://doi.org/10.1029/2017MS001217>)

- 582 New M, Lister D, Hulme M and Makin I (2002) A high-resolution data set of surface climate over global land areas.
583 *Climate Research*, **21**(1), 1–25 (doi: 10.3354/cr021001)
- 584 Oerlemans J and Fortuin J (1992) Sensitivity of glaciers and small ice caps to greenhouse warming. *Science*, **258**(5079),
585 115–117
- 586 Oerlemans J and Reichert B (2000) Relating glacier mass balance to meteorological data by using a seasonal sensitivity
587 characteristic. *Journal of Glaciology*, **46**(152), 1–6
- 588 OGGM (2022) Oggm edu. <https://edu.oggm.org/en/latest/>, accessed: 2022-12-20
- 589 Ohmura A (2001) Physical basis for the temperature-based melt-index method. *Journal of applied Meteorology*, **40**(4),
590 753–761
- 591 O'Neill BC, Tebaldi C, van Vuuren DP, Eyring V, Friedlingstein P, Hurtt G, Knutti R, Kriegler E, Lamarque JF,
592 Lowe J, Meehl GA, Moss R, Riahi K and Sanderson BM (2016) The scenario model intercomparison project
593 (scenariomip) for cmip6. *Geoscientific Model Development*, **9**(9), 3461–3482 (doi: 10.5194/gmd-9-3461-2016)
- 594 Pertziger F (1996) Abramov glacier data reference book: climate, runoff, mass balance. *Central Asian Regional*
595 *Research Hydrometeorological Institute, Tashkent, Republic of Uzbekistan*
- 596 Pradhananga D, Pomeroy JW, Aubry-Wake C, Munro DS, Shea J, Demuth MN, Kirat NH, Menounos B and Mukher-
597 jee K (2021) Hydrometeorological, glaciological and geospatial research data from the peyto glacier research basin
598 in the canadian rockies. *Earth System Science Data*, **13**(6), 2875–2894
- 599 Prudhomme C, Wilby RL, Crooks S, Kay AL and Reynard NS (2010) Scenario-neutral approach to climate change
600 impact studies: application to flood risk. *Journal of Hydrology*, **390**(3-4), 198–209
- 601 Reilly J, Stone PH, Forest CE, Webster MD, Jacoby HD and Prinn RG (2001) Uncertainty and climate change
602 assessments
- 603 RGI Consortium (2017) Randolph Glacier Inventory (RGI) – A Dataset of Global Glacier Outlines: Version 6.0.
604 Technical Report, Global Land Ice Measurements from Space (doi: /10.7265/N5-RGI-60)
- 605 Seland Ø, Bentsen M, Olivié D, Toniazzo T, Gjermundsen A, Graff LS, Debernard JB, Gupta AK, He YC, Kirkevåg
606 A, Schwinger J, Tjiputra J, Aas KS, Bethke I, Fan Y, Griesfeller J, Grini A, Guo C, Ilicak M, Karset IHH, Landgren
607 O, Liakka J, Moseid KO, Nummelin A, Spensberger C, Tang H, Zhang Z, Heinze C, Iversen T and Schulz M (2020)
608 Overview of the norwegian earth system model (noresm2) and key climate response of cmip6 deck, historical, and
609 scenario simulations. *Geoscientific Model Development*, **13**(12), 6165–6200 (doi: 10.5194/gmd-13-6165-2020)

- 610 Shea JM and Marshall SJ (2007) Atmospheric flow indices, regional climate, and glacier mass balance in the canadian
611 rocky mountains. *International Journal of Climatology: A Journal of the Royal Meteorological Society*, **27**(2), 233–
612 247
- 613 Singh S, Kumar R and Dimri A (2018) Mass balance status of indian himalayan glaciers: A brief review. *Frontiers*
614 *in Environmental Science*, **6**, 30
- 615 Slangen A, Adloff F, Jevrejeva S, Leclercq P, Marzeion B, Wada Y and Winkelmann R (2017) A review of recent
616 updates of sea-level projections at global and regional scales. *Integrative Study of the Mean Sea level and Its*
617 *Components*, 395–416
- 618 Strasser U, Marke T, Braun L, Escher-Vetter H, Juen I, Kuhn M, Maussion F, Mayer C, Nicholson L, Niedertscheider
619 K and others (2018) The rofental: a high alpine research basin (1890–3770 m asl) in the ötztal alps (austria) with
620 over 150 years of hydrometeorological and glaciological observations. *Earth System Science Data*, **10**(1), 151–171
- 621 Switzerland GM (2022) Glamos: Glamos web page. <https://www.foto-webcam.eu/webcam/hintereisferner1/>,
622 accessed: 2022-12-20
- 623 Ultee L, Coats S and Mackay J (2022) Glacial runoff buffers droughts through the 21st century. *Earth System*
624 *Dynamics*, **13**(2), 935–959
- 625 van der Laan L, Förster K, Scaife A, Vlug A and Maussion F (2022) Assessing skill and use of cmip6 decadal
626 re-forecasts in global glacier mass balance modelling. Technical report, Copernicus Meetings
- 627 Van Vuuren DP, Stehfest E, den Elzen MG, Kram T, van Vliet J, Deetman S, Isaac M, Klein Goldewijk K, Hof A,
628 Mendoza Beltran A and others (2011) Rcp2. 6: exploring the possibility to keep global mean temperature increase
629 below 2 c. *Climatic change*, **109**(1), 95–116
- 630 WGMS (2022a) Fluctuations of glaciers database. World Glacier Monitoring Service, Zurich, Switzerland. (doi:
631 10.5904/wgms-fog-2022-09)
- 632 WGMS (2022b) Reference glaciers for mass balance. https://wgms.ch/products_ref_glaciers/, accessed: 2022-
633 12-01
- 634 Wijngaard RR, Steiner JF, Kraaijenbrink PD, Klug C, Adhikari S, Banerjee A, Pellicciotti F, Van Beek LP, Bierkens
635 MF, Lutz AF and others (2019) Modeling the response of the langtang glacier and the hintereisferner to a changing
636 climate since the little ice age. *Frontiers in Earth Science*, **7**, 143
- 637 Young G (1981) The mass balance of peyto glacier, alberta, canada, 1965 to 1978. *Arctic and Alpine Research*, **13**(3),
638 307–318

- 639 Zemp M, Hoelzle M and Haeberli W (2009) Six decades of glacier mass-balance observations: a review of the
640 worldwide monitoring network. *Annals of Glaciology*, **50**(50), 101–111
- 641 Zemp M, Huss M, Thibert E, Eckert N, McNabb R, Huber J, Barandun M, Machguth H, Nussbaumer SU, Gärtner-
642 Roer I and others (2019) Global glacier mass changes and their contributions to sea-level rise from 1961 to 2016.
643 *Nature*, **568**(7752), 382–386

For Peer Review